Chalcogenide Letters Vol. 15, No. 6, June 2018, p. 327 - 337

INFLUENCE OF DEPOSITION PARAMETERS ON THE MORPHOLOGY, STRUCTURAL AND OPTICAL PROPERTIES OF Cu_2ZnSnS_4 THIN FILMS GROWN BY SOLVOTHERMAL METHOD

H. ZHENG[a], A. WEI[a, b,*], H. XIONG[a]
[a] *Guangdong Provincial Key Laboratory of Functional Soft Condensed Matter, School of Material and Energy, Guangdong University of Technology, Guangzhou 510006, China*
[b] *Department of Information Science，Xin Hua College of Sun Yat-Sen University, Guangzhou 510520, China*

In this study, the Cu_2ZnSnS_4 (CZTS) thin films have been directly grown on transparent conductive fluorine-doped tin oxide (FTO) substrates via a solvothermal synthetic route. The effects of deposition temperature and deposition time on the morphology, structure, composition and optical properties of CZTS thin films were investigated using scanning electronic microscopy (SEM), X-ray diffraction (XRD), Raman spectroscopy, energy dispersive spectrometry (EDS) and UV-visible spectrophotometry, respectively. The results indicated that the deposition temperature obviously affect crystal structures, surface morphology and composition of CZTS thin films. The thin films are mainly composed of CZTS with kesterite phase, however it contains a little binary and ternary impurities phase especially for samples prepared at low temperatures of 140℃ and 170℃. The CZTS thin films prepared at temperatures of 140℃ and 170℃ are composed of a large number of sphere-like particles with an average diameter of about 300-450 nm. The CZTS thin films grown at 200°C are composed of vertically oriented nano-flakes which directly spread over the FTO substrates. The deposition time do not obviously affect crystal structures and morphology. The crystallite sizes of CZTS thin films increase gradually with deposition temperature raising or deposition time prolonging. The strong absorption in the visible light region and a band gap of approximately 1.5 eV suggest that the CZTS thin films can be used as an absorber layer of thin film solar cells.

(Received March 7, 2018; Accepted June 5, 2018)

Keywords: Semiconductors, Solvothermal method, Cu_2ZnSnS_4 thin films, Optical properties

1. Introduction

Chalcogenide materials, such as CuInSe, $CuIn_xGa_{1-x}Se_2$, CdTe, PbTe, etc., have been of interest for application in the fields of photovoltaic, photocatalysis and thermoelectric [1-3]. However, due to the limitation of the rarity of indium (In) and tellurium (Te) and the toxicity of cadmium (Cd), it has increased attention on developing earth-abundant, inexpensive and environment friendly chalcogenide materials [4-6]. As a novel energy conversion material, Cu_2ZnSnS_4 (CZTS) has been proposed as absorber materials to substitute $CuIn_xGa_{1-x}Se_2$ (CIGS) for thin film solar cells due to its relatively large absorption coefficient of 10^4 cm^{-1} in visible spectrum range, an optimum direct band gap energy of 1.5 eV, p-type conductivity, low toxicity, high photovoltaic efficiency, and relatively high abundance of its constituent elements [7-10]. The reported power conversion efficiency (PCE) of CZTS -based solar cells were achieved to 8.4%, 12.6% and 7.2%, respectively, based on vacuum deposited technique [11], solution-processed method [12] and nanocrystal inks approach [13]. While theoretically predicted maximum power conversion efficiency for CZTS -based solar cells was 32.4% [14, 15]. Therefore, a great amount of work has to be done in order to bring the power conversion efficiency closer to the theoretical limit. It is well recognized that the key challenges of CZTS material for solar cell applications are sophisticated phase and composition finely control synthesis. Unlike its analogous CdTe or

* Corresponding author. weiax@gdut.edu.cn

$CuIn_xGa_{1-x}Se_2$, single-phase kesterite CZTS exists only within a narrow stoichiometry range [16, 17]. The presence of volatile elemental constituents [18], binary phases [19, 20] and harmful point defects further complexes the phase purity issue within the deposited films, particularly under high temperatures and vacuum conditions. Thus, the exquisite controllability over composition [21, 22] and phase become the key prerequisite in any synthetic routes for the fabrication of high performance CZTS films solar cells.

Several different solution-based approaches to synthesize CZTS have been studied, for example, the spray pyrolysis [23], the sol–gel method [24], microwave-assisted solution methods [25], hot-injection solution synthesis method [26], and solvothermal method [27]. Compared to these techniques, the solvothermal method can be regarded as a powerful tool for the controllable synthesis of semiconductor nanocrystals. The main advantages of solvothermal synthesis are not only facile, high purity, low-cost and environmental-friendly but also high-yield, high-crystalline, energy-saving and controllable.

In this work, we describe a simple solvothermal method for direct growth of CZTS thin films on FTO substrate. The effects of deposition temperature and deposition time on the morphology, structure, composition and optical properties of CZTS thin films were studied.

2. Experimental details

2.1 Facile synthesis of CZTS thin films

The FTO glass substrates were cut into pieces of 10 x 20 mm cleaned ultrasonically in acetone, alcohol and de-ionized water for 10 min each prior to synthesis. All the reagents were analytical grade and they were used as starting materials without any further purification. The CZTS thin films were directly grown on FTO substrates by facile solvothermal method. A typical synthetic procedure of CZTS thin films is brief described below. First, 1 mmol of copper (II) chloride dihydrate ($CuCl_2 \cdot 2H_2O$), 2 mmol of zinc (II) chloride ($ZnCl_2$) , 0.5 mmol of tin (II) chloride dehydrate ($SnCl_2 \cdot 2H_2O$), 10 mmol of thiourea (CH_4N_2S), 0.25 mmol of hexadecyl trimethyl ammonium Bromide (CTAB) and 2.8 mmol of oxalic acid ($H_2C_2O_4$) were dissolved, mixed and stirred in 40 ml of ethanol as the precursor solution. Secondly, the well-cleaned FTO substrates were placed inside the Teflon liner, conducting side facing down with an angle of about 35°-40° against the wall. The precursor solution was added into the Teflon liner of 60 ml capacity, and the Teflon liner was loaded in a stainless steel autoclave. The stainless-steel autoclave was sealed and put into an electric oven. Thirdly, the solvothermal process was conducted for 24 hours at temperatures 140°C, 170°C, 200°C and 230°C, respectively. Another series samples were prepared at temperature 200°C for 5, 10, 15 and 20 hours, respectively. Thereafter, the autoclave was cooled down to room temperature naturally. The CZTS thin films grown on FTO substrates were then rinsed with deionized water and subsequently dried in the ambient. The deposition process parameters for two series samples were listed in Table 1.

Table 1 Deposition process parameters of CZTS thin films.

Sample No.	$CuCl_2$ mmol	$ZnCl_2$ mmol	$SnCl_2$ mmol	CH_4N_2S mmol	CTAB mmol	$H_2C_2O_4$ mmol	Ethanol ml	Temperature ^oC	Time h
A1	1	2	0.5	10	0.25	2.8	40	140	20
A2	1	2	0.5	10	0.25	2.8	40	170	20
A3	1	2	0.5	10	0.25	2.8	40	200	20
A4	1	2	0.5	10	0.25	2.8	40	230	20
B0	1	2	0.5	10	0.25	2.8	40	200	1
B1	1	2	0.5	10	0.25	2.8	40	200	5
B2	1	2	0.5	10	0.25	2.8	40	200	10
B3	1	2	0.5	10	0.25	2.8	40	200	15
B4	1	2	0.5	10	0.25	2.8	40	200	20

2.2 Characterization of CZTS thin films

The phase structure of CZTS thin films was analyzed using X-ray diffraction (XRD, D/MAXUltima χ, Rigaku) and laser Raman spectroscopy (Renishaw, 514.5nm). XRD patterns were obtained using a CuK_α radiation source over diffraction angles ranging from 20° to 80° at a scanning speed of 6° min^{-1} with a grazing angle of 0.5°. The morphologies of CZTS thin films were examined using a field-emission scanning electron microscopy (FE-SEM, SU8010, Hitachi). The chemical composition analysis was performed by energy dispersive X-ray spectroscopy (EDX). UV-Vis-NIR transmission spectrum was recorded on a T6 spectrophotometer in the wavelength range of 400–1000 nm.

3. Results and discussion

3.1 Effect of deposition temperature and deposition time on morphology of CZTS thin films

The SEM images of the CZTS thin films grown at different deposition temperatures are shown in Fig. 1. The deposition temperatures obviously affect the surface morphology and microstructure of CZTS thin films. For sample A1 grown at temperature of 140°C, the CZTS thin films are composed of a large number of sphere-like particles, and the average diameter of spherical particles is about 450 nm. The surface of sphere-like particles seems to be considerably rough. For sample A2 grown at temperature of 170°C, the CZTS films are also composed of a large of uniform and densely packed sphere-like particles which are formed by many gathering together nano-flakes. The average diameter of sphere-like particles is about 300 nm. However, the morphology and microstructure of CZTS thin films grown at 200°C are different from that of CZTS thin films grown at 140°C and 170°C. The CZTS thin films are composed of vertically oriented nano-flakes which directly spread over the FTO substrates. These nano-flakes interconnect with each other to form an entangled network-like architecture, meanwhile, a few flower-like microspheres gathering by nano-flakes also are observed. When deposition temperature is raised to 230°C (sample A4), the CZTS thin films could be seen as consisting of sphere-like particles, but these sphere-like particles are made up of a large number of nanorods with length of 200 nm and diameter of 20nm.

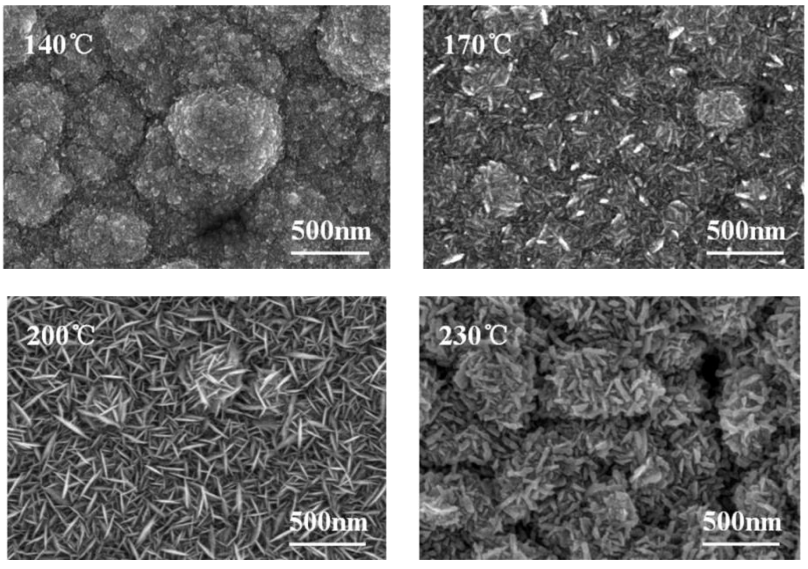

Fig. 1 SEM images of CZTS thin films prepared at different depositin temperature.

To further understand the formation process and growth mechanism for CZTS thin films, detailed morphology as a function of growth time are studied using SEM. Fig.2 shows SEM images of the CZTS thin films grown on the FTO substrate with growth time of 1, 5, 10, 15 and 20

hours while the reaction solution and deposition temperature are kept the same as that of sample A3. After a shorter deposition time of 1 hour, no any formations (product) is observed on surface of FTO substrate, which should be that the precursor solution has not reached the high temperature and high pressure conditions required for the reaction. When the deposition times are prolonged to 5 hours, the small particles composing of nano-flakes are formed on the surface of the FTO substrate, as indicated in Fig. 2 (b). These dense and tiny particles act as nucleation sites to induce the growth of the nano-flakes CZTS thin films. When the times increase to 10 hours, 15 hours and 20 hours, The CZTS thin films are composed of vertically oriented nano-flakes which directly spread over the FTO substrates and the size of nano-flakes gradually grows up with the deposition time prolonging. The thickness of CZTS thin films is 600 nm when deposition times reach 20 hours.

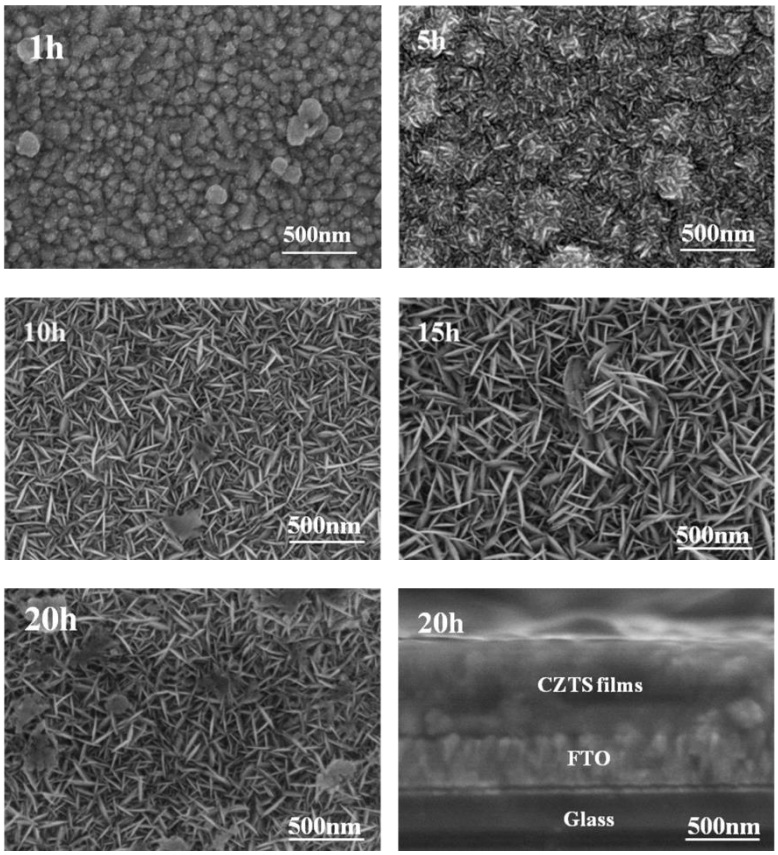

Fig. 2 SEM images of CZTS thin films prepared at different deposition time.

3.2 Effect of deposition temperature and deposition time on structure of CZTS thin films

The XRD patterns of CZTS thin films prepared at different deposition temperature and deposition time are shown in Fig.3 (a) and (b), respectively. Except for peaks from the FTO substrate (marked by♦), The diffraction peaks appearing at 2θ= 28.53 °, 32.98 °, 47.33 ° and 56.17 ° can be indexed (112), (200), (220) and (312) of the kesterite crystal structure (JCPDS No. 26-0575) of stoichiometric CZTS [28]. No obvious peaks resulting from binary and ternary impurities phases, such as ZnS, SnS_2, $Cu_{2-x}S$, Cu_3SnS_4, and Cu_2SnS_3 etc. are observed. According to the well-known Debye–Scherrer equation, the average crystallite size can be calculated as:

$$D = \frac{K\lambda}{\beta \cos\theta} \tag{1}$$

where D is the average crystallite size, λ is the wavelength of the x-ray radiation used, β is the

full-width at half-maximum intensity of the peak, θ is the angle at which the diffraction peak occurs, and K is Scherrer constant. In calculating the crystallite size, the value of K is taken as 0.94. The Scherrer constant K depends on how the width is determined, the shape of the crystal and the size distribution. The most common values for K are: (1) 0.94 for the FWHM of spherical crystals with cubic symmetry and (2) 0.89 for the integral breadth of spherical crystals with cubic symmetry. From the preferred (112) diffraction peaks, the estimated crystallite sizes of the CZTS thin films prepared using various process parameters are listed in Table 2. They are 4.25 nm, 8.16 nm, 12.53 nm and 13.17 nm for samples A1, A2, A3 and A4, and they are 6.71 nm, 11.91 nm, 13.97 nm and 13.17 nm for samples B1, B2, B3 and B4, respectively. The results indicate that the intensity of diffraction peaks of (112) plane and the crystallite sizes of CZTS thin films increases gradually with deposition temperature raising or deposition time prolonging.

XRD is generally used as the main tool to analyze the structure of such compounds, but it is not sufficient to identify most of the minor phases, since cubic ZnS (JCPDS No.5-0566) and tetragonal Cu_2SnS_3 (JCPDS No.89-4714) have very similar diffraction pattern with tetragonal CZTS. Hence, Raman spectroscopy was used to further confirm the phase purity of as-synthesized CZTS thin films. Raman spectra of CZTS thin films prepared at different deposition temperature and deposition time are shown in Fig.3 (c) and (d), respectively. The Raman spectrum of CZTS thin films prepared at 140-230℃ exhibits intense peak at 336 cm^{-1} and two shoulders at 295 cm^{-1} and 371 cm^{-1} which match well with the reported values of kesterite structure CZTS [27]. The strong peak at 336 cm^{-1} arises from A1 vibration mode of lattice, where the group VI atoms (S) vibrate while the rest of atoms (Cu, Zn and Sn) remain fixed. Meanwhile, the weak peak at 318 cm^{-1} is also observed. In addition, the weak peaks at 251 cm^{-1} and 425 cm^{-1} are observed for sample grown at 140℃. As seen in Fig. 3(c), the broad peaks centered at around 295 cm^{-1} and 336 cm^{-1} can be considered as the superimposed spectrums of tetragonal CZTS (290 cm^{-1} and 332 cm^{-1} [29, 30]), tetragonal Cu_2SnS_3 (297 cm^{-1} and 352 cm^{-1} [29, 30]) , and orthorhombic Cu_2SnS_3(318 cm^{-1}). The peaks at 250 cm^{-1} and 475 cm^{-1} can be assigned $Cu_{2-x}S$ [29, 30]. According to the results of XRD and Raman data, the samples prepared by solvothermal method are mainly composed of CZTS, however it contains a little binary and ternary impurities phase of ZnS, SnS, $Cu_{2-x}S$ and Cu_2SnS_3, especially for samples prepared at low temperatures of 140℃ and 170℃. As seen from Fig.3(d), for samples prepared at deposition temperature of 200℃ with growth time of 5 hours, 10 hours, 15 hours and 20 hours, Raman spectra mainly show the peaks centered at 295 cm^{-1} and 336 cm^{-1}, and the intensity of peaks from impurities phase is very weak. The intensity of peak at 336 cm^{-1} increases gradually with deposition time prolonging, which mainly ascribed to the crystallite size of CZTS thin films increase gradually.

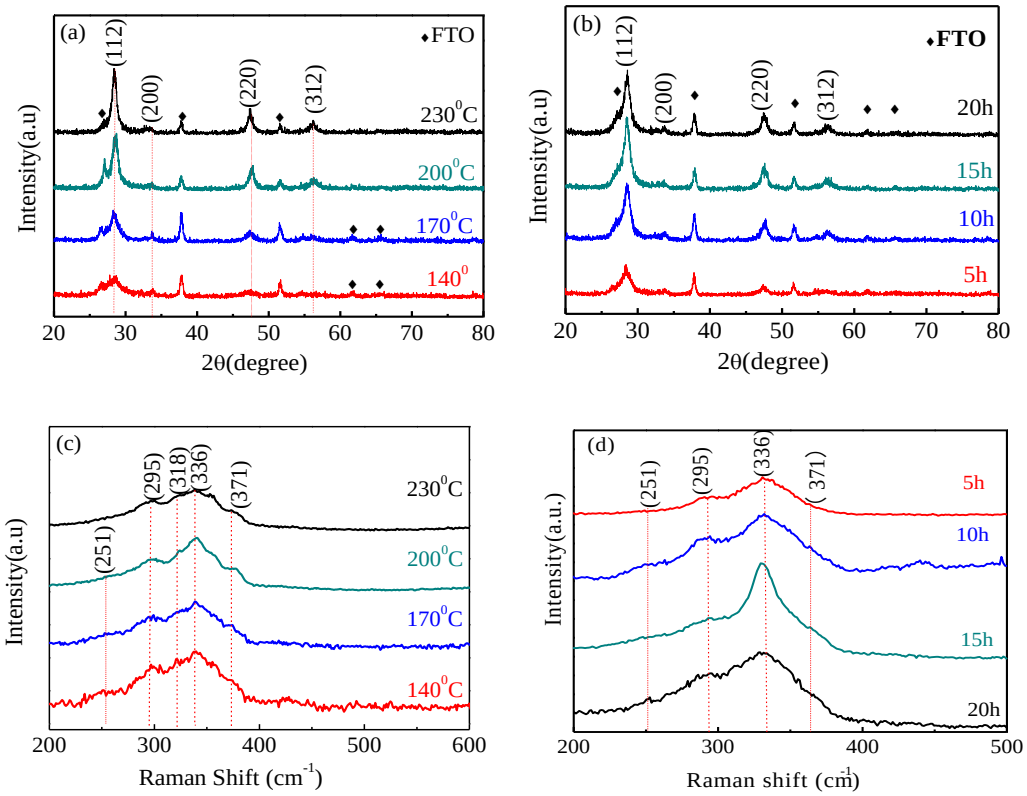

Fig. 3 (a) XRD patterns and (c) Raman spectra of the CZTS thin films prepared at different deposition temperature; (b) XRD patterns and (d) Raman spectra of the CZTS thin films prepared at different deposition time.

3.3 Effect of deposition temperature and deposition time on composition of CZTS thin films

To obtain the composition information of the CZTS thin films, the elemental analysis of the as-synthesized CZTS thin films was performed using the EDS technique. The contents of Cu, Zn, Sn, S and Cu/Zn, S/Cu, Cu/Zn/Sn/S atomic ratios of various samples are listed in Table 2. Although EDS is a semi-quantitative analysis technique, the following conclusions could be drawn. Firstly, the amounts of thiourea in the precursor solution are much more than the stoichiometric values required, the S content of CZTS thin films is much lower than the ideal target value. This indicates that thiourea is not exhausted after reactions. Secondly, the Sn contents is more than Zn contents for most samples, which may be partly ascribed to FTO substrate containing Sn element, partly ascribed to Zn source showing lower reactivity than Sn and Cu sources . Thirdly, as seen from Raman spectrum of CZTS thin films, the presence of a little $Cu_{2-x}S$ and Cu_3SnS_4 in CZTS thin films is another possible reason for the Cu rich and Zn poor for samples prepared at low temperature of 140°C and 170°C (A1 and A2) and sample prepared at 200°C with deposition time of 5 hours (B1). The ideal stoichiometry of CZTS requires that the atomic ratios of Cu/ (Zn+Sn) and Zn/Sn equal to 1. However, Katagiri et al [8] suggest that the atomic ratios of Cu/ (Zn+Sn) and Zn/Sn near to 0.85 and 1.25 respectively show good optoelectronic properties and best device efficiency.

Table 2 Atom ratios, grain size and optical band gap of various samples.

Sampls No.	Cu at.%	Zn at.%	Sn at.%	S at.%	Cu/Zn	S/Cu	Cu/Zn/Sn/S	grain size nm	optical gap eV
A1	28.5	12.4	19.7	39.4	2.30	1.38	2.3: 1.0: 1.6: 3.2	4.25	1.58
A2	30.9	13.9	17.2	38.0	2.22	1.23	2.2: 1.0: 1.2: 2.7	8.16	1.54
A3	28.1	15.3	13.4	43.2	1.84	1.54	1.8: 1.0: 0.9: 2.8	12.53	1.52
A4	26.4	13.0	15.3	45.3	2.03	1.72	2.0: 1.0: 1.2: 3.5	13.17	1.53
B1	33.2	8.5	20.4	37.9	3.92	1.14	3.9: 1.0: 2.4: 4.5	6.71	1.63
B2	25.3	12.6	18.1	44.0	2.01	1.74	2.0: 1.0: 1.4: 3.5	11.91	1.60
B3	28.3	16.9	15.7	39.1	1.67	1.38	1.7: 1.0: 0.9: 2.3	13.97	1.50
B4	29.6	15.3	14.9	40.2	1.93	1.34	1.9: 1.0: 1.0: 2.6	13.17	1.52

Fig.4 shows the SEM-EDS elemental mapping of sample A3. The element of Cu, Zn, Sn, and S exist in the sample. As can be seen form Fig.4, the distribution of elements Cu, Sn and S is uniform. However, the distribution of elements Zn is not uniform. Reaction and growth mechanism of the CZTS thin films has been discussed in detail in our previous works [31]. The whole formation process of CZTS thin films involves three steps. First, Cu^{2+}, Zn^{2+}, and Sn^{4+} coordinate with thiourea (Tu) molecules to form M-thiourea complexes ($[Cu(Tu)_n(H_2O)_x]^{2+}$, $[Zn(Tu)_n(H_2O)_x]^{2+}$ and $[Sn(Tu)_n(H_2O)_x]^{4+}$) in reactive solution [28]. When all reagents are dissolved, mixed and stirred in ethanol, the colors of the precursor solution change from green-blue to colorless transparent solution, which confirms the formation of metal-thiourea (Tu) complexes. Secondly, $[Cu(Tu)_n(H_2O)_x]^{2+}$ is deoxidized by oxalic acid and formed the reduced product $[Cu(Tu)_n(H_2O)x]^{+}$. Meanwhile, at the solvothermal temperature, Tu reacts with the trace water introduced by the solvent or hydrated metal salt and produces hydrogen sulfide, and hydrogen sulfide decompose into S^{2-} and H^{+} ions. Finally, M-Tu complexes react with S^{2-} to form the final product CZTS. Because the Zn^{2+} ions show lower reactivity than the Cu^{2+} and Sn^{4+} ions, Tu is prior to coordinate with Cu^{2+} and Sn^{4+} ions to form $[Cu(Tu)_n(H_2O)_x]^{2+}$ and $[Sn(Tu)_n(H_2O)_x]^{4+}$ complexes in reactive solution. When Cu^{2+} is reacted completely, Zn^{2+} ions is easier to coordinate with thiourea to form $[Zn(Tu)_n(H_2O)_x]^{2+}$. So, deposition temperature raising or deposition time prolonging leads to the decreasing of Cu/Zn atom ratio in CZTS thin films. Based on this result, we infer that stoichiometic Cu_2ZnSnS_4 thin films could be synthesized using solvothermal method by properly controlling the ratio of different reaction agent and deposition temperature.

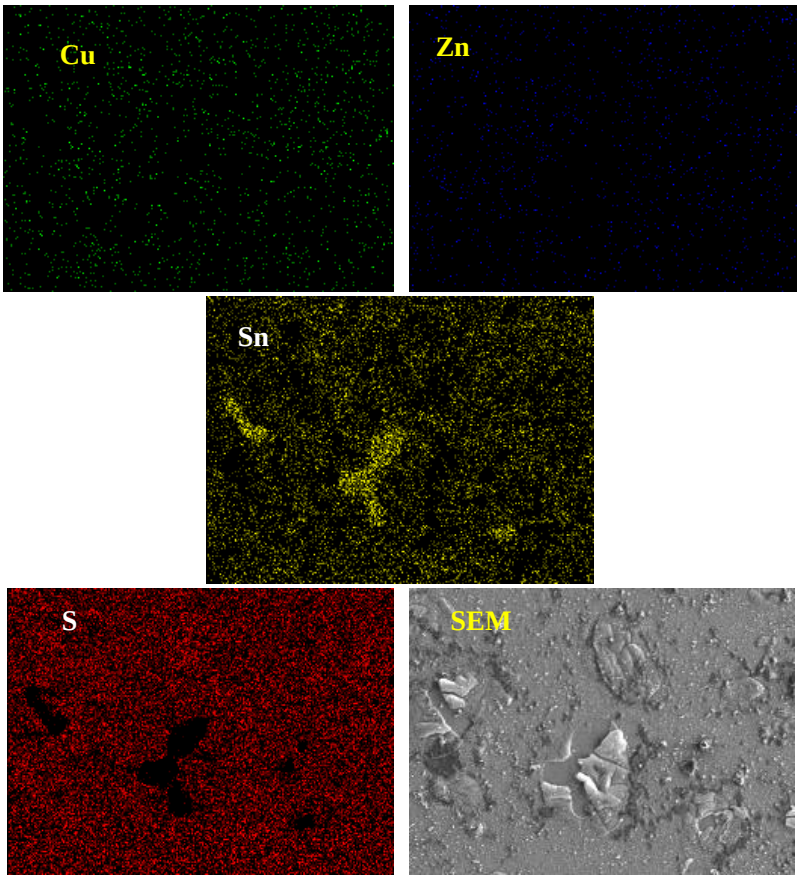

Fig. 4 SEM image and energy dispersive X-ray spectroscopy (EDS) elemental maps of sample A3.

3.4 Effect of deposition temperature and deposition time on optical property of CZTS thin films

Fig.5 (a) and (b) show the optical transmission spectra in the wavelength range of 400 to 1000 nm of the CZTS thin films deposited using different deposition temperature and different deposition time. From the transmission spectra, the values of the absorption coefficient α are calculated using the relation:

$$\alpha = \frac{1}{d} \ln\left(\frac{1}{T}\right) \tag{2}$$

where d is thickness and T is transmittance of CZTS thin films. The thickness of the thin films is determined from cross-sectional view of SEM images. The absorption coefficient α for a direct band gap material can be related to the photon energy $h\nu$ by the Tauc relation:

$$\alpha = \frac{B(h\nu - E_g)^{\frac{1}{2}}}{h\nu} \tag{3}$$

where $h\nu$ is the photon energy, E_g is the band gap, B is a constant. Relation (3) can be further written as the following form:

$$(\alpha h\nu)^2 = A(h\nu - E_g) \tag{4}$$

Fig. 5 (c) and (d) show the plots of $(\alpha h\nu)^2$ as a function of $h\nu$ which is corresponding to the optical transmission spectra in Fig.5 (a) and (b), respectively. Extrapolation of the linear portion of the curves to $(\alpha h\nu)^2 = 0$ gives the optical band gap E_g. The optical band gaps are extracted to be 1.58 eV, 1.54 eV, 1.52 eV, and 1.53 eV for samples A1, A2, A3 and A4, respectively; they are 1.63 eV, 1.60 eV, 1.50 eV and 1.52 eV for sample B1, B2, B3 and B4, respectively. For samples prepared at low temperature of 140°C (A1) and samples prepared at 200°C with deposition time of 5 hours and 10 hours (B1, B2), the value optical band gap is larger than that of other samples, which may be ascribed to the existence of impurities phase in the samples. Since the presence of secondary phases like ZnS (3.6 eV) will increase the band gap of the synthesized CZTS thin films. The strong absorption in the visible light region and a band gap of approximately 1.5 eV suggest that the CZTS thin films can be used as an absorber layer of thin film solar cells.

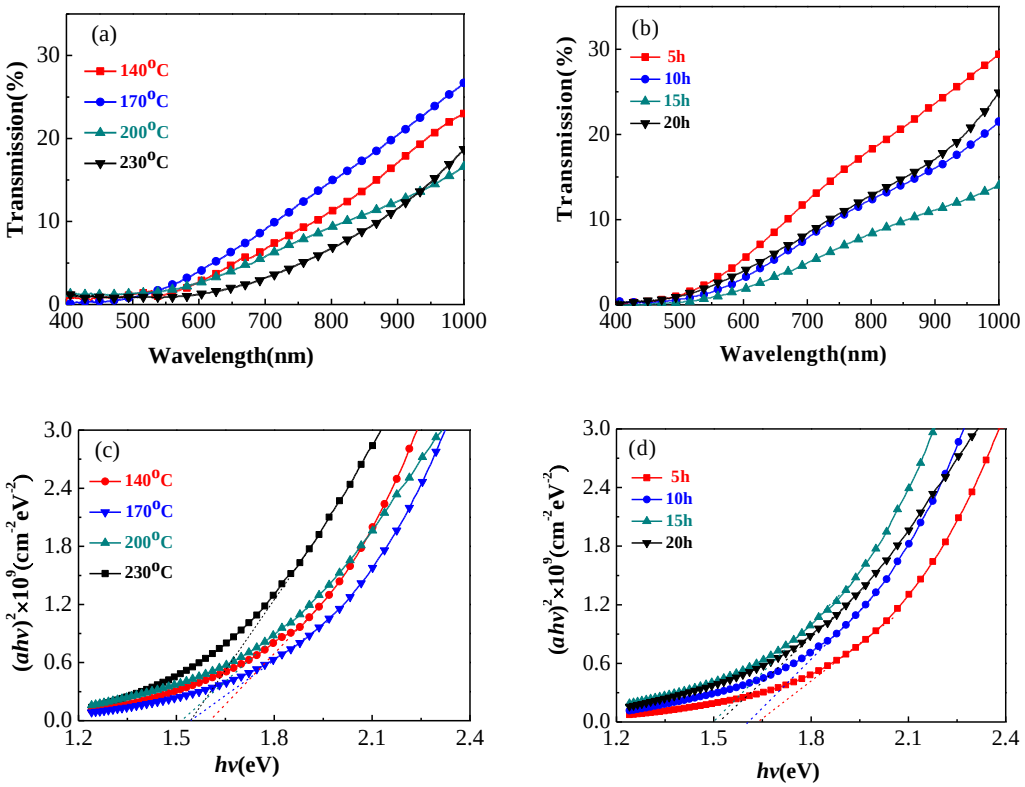

Fig.5 (a) UV-Vis transmission spectrum and (c) $(\alpha hv)^2$-hv curves of the CZTS thin films prepared at different deposition temperature; (b) UV-Vis transmission spectrum and (d) $(\alpha hv)^2$-hv curves of the CZTS thin films prepared at different deposition time.

4. Conclusions

In summary, the CZTS thin films are successfully prepared on FTO substrates by one-step solvothermal method. For CZTS thin films prepared at temperature of 140°C and 170 °C are in the kesterite structure with a little binary and ternary impurities phase, composed of a large number of uniform sphere-like particles with an average diameter of about 300-450 nm. The existence of the impurities phase in the samples results in Cu rich, Zn and S poor. The CZTS thin films prepared at temperature of 200°C are composed of vertically oriented nano-flakes which directly spread over the FTO substrates, and Cu: Zn: Sn: S atomic ratio is closer to the theoretical value of 2:1:1:4 of stoichiometric Cu_2ZnSnS_4. The deposition times do not obviously affect surface morphology and crystal structures, but affect the Cu: Zn: Sn: S atom ratio and optical band gap of CZTS thin films. The optimal growth conditions for CZTS thin films are deposition temperature of 200°C and deposition time of 15 hours. The strong absorption in the visible light region and a band gap of

approximately 1.5 eV suggest that the CZTS thin films can be used as an absorber layer of thin film solar cells.

Acknowledgements

This work has been financially supported by the Science and Technology Program of Guangdong Province of China (No. 2016A010104020), the Training Plan of Outstanding Young Teachers of Universities in Guangdong Province (Grant No. YQ2015055) and Pearl River S&T Nova Program of Guangzhou (Grant No. 201610010116).

References

[1] J. S. Luo, S. D. Tilley, L. Steier, M. Schreier, M. T. Mayer, H. J. Fan, M. Grätzel, Nano. Lett. **15**, 1395 (2015).
[2] X. G. Huang, Z. Zhang, B. Song, Y. L. Deng, S. Liu, Y. Cui, G. Wang, C. P. Wong, J. Alloys Compd. **656**, 663 (2016).
[3] M. A. Hossain, M. Q. Wang, K. L. Choy, ACS Appl. Mater. Interfaces **7**, 22497 (2015).
[4] S. Sarkar, B. Das, P. R. Midya, G. C. Das, K. K. Chattopadhyay, Mater. Lett. **152**, 155 (2015).
[5] A. Kamble, K. Mokurala, A. Gupta, S. Mallick, P. Bhargava, Mater. Lett. **137**, 440 (2014).
[6] Y. A. Jadhav, P. R. Thakur, S. K. Haram, Sol. Energy Mat. Sol. C. **155**, 273 (2016).
[7] Z. Hao, Z. Zhang, S. Liu, Y. Cui, Mater. Lett. **183**, 268 (2016).
[8] H. Katagiri, K. Jimbo, W.S. Maw, K. Oishi, M. Yamazaki, H. Araki, A. Takeuchi, Thin Solid Films **517**, 2455 (2009).
[9] A. Khare, A.W. Wills, L.M. Ammerman, D.J. Norris, E.S. Aydil, Chem. Commun. **47**, 11721 (2011).
[10] D. B. Mitzi, O. Gunawan, T. K. Todorov, K. J. Wang, S. Guha, Sol. Energy Mat. Sol. C. **95**, 1421 (2011).
[11] B. Shin, O. Gunawan, Y. Zhu, N. A. Bojarczuk, S. J. Chey, S. Guha, Prog. Photovolt.: Res. Appl. **21**, 72 (2013).
[12] W. Wang, M. T. Winkle, O. Gunawan, T. Gokmen, T. K. Todorov, Y. Zhu, D. B. Mitzi, Adv. Energy Mater. **4**, 1301465 (2014).
[13] Q. J. Guo, G. M. Ford, W. C. Yang, B. C. Walker, E. A. Stach, H. W. Hillhouse, R. Agrawal, J. Am. Chem. Soc. **132,** 17384 (2010).
[14] Y. L. Zhou, W. H. Zhou, Y. F. Du, M. Li, S. X. Wu, Mater. Lett. **65**, 1535 (2011).
[15] L. Shi, C. J. Pei, Y. M. Xu, Q. Li， J. Am. Chem. Soc. **133**, 10328 (2011).
[16] C. Wang, S. Chen, J. H. Yang, L. Lang, H. J. Xiang, X. G. Gong, A. Walsh, S. H. Wei, Chem. Mater. **26**, 3411 (2014).
[17] A. D. Collord, H. W. Hillhouse, Chem. Mater. **27**, 1855 (2015).
[18] M. Kumar, A. Dubey, N. Adhikari, S. Venkatesanb, Q. Qiao, Energy Environ. Sci. **8**, 3134 (2015).
[19] J. M. R. Tan, Y. H. Lee, S. Pedireddy, T. Baikie, X. Y. Ling, L. H. Wong, J. Am. Chem. Soc. **136**, 6684 (2014).
[20] Q. Guo, G. M. Ford, W. C. Yang, C. J. Hages, H. W. Hillhouse, R. Agrawal, Sol. Energy Mater. Sol. C. **105**, 132 (2012).
[21] F. J. Fan, L. Wu, M. Gong, G. Liu, Y. X. Wang, S. H. Yu, S. Chen, L. W. Wang, X. G. Gong, ACS nano. **7**, 1454 (2013).
[22] S. Bahramzadeh, H. Abdizadeh, M. R. Golobostanfard, J. Alloys Compd. **642**, 124 (2015).
[23] N. M. Shinde, R. J. Deokate, C. D. Lokhande, J. Anal. Appl. Pyrol. **100**, 12 (2013).
[24] Z. H. Su, K. W. Sun, Z. L. Han, H. T. Cui, F. Y. Liu, Y. Q. Lai, J. Li, X. J. Hao, Y. X. Liu, M. A. Green, J. Mater. Chem. A. **2**, 500 (2014).

[25] W. Wang, H. L. Shen, X. C. He, Mater. Res. Bull. **48**, 3140 (2013).
[26] X. T. Lu, Z. B. Zhuang, Q. Peng, Y. D. Li, Chem. Commun. **47**, 3141 (2011).
[27] M. Pal, N. R. Mathews, R. S. Gonzalez, X. Mathew, Thin Solid Films **535**, 78 (2013).
[28] Y. L. Zhou, W. H. Zhou, M. Li, Y. F. Du, S. X. Wu, J Phys Chem C. **115**, 19632 (2011).
[29] P. R. Ghediya, T. K. Chaudhuri, J. Mater. Sci.: Mater. Electron. **26**, 1908 (2015).
[30] P. A. Fernandes, P. M. P. Salomé, A. F. Cunha, J. Alloys Compd. **509**, 7600 (2011).
[31] A. X. Wei, Z. Yan, Y. Zhao, M. X. Zhuang, J. Liu, Int. J. Hydrogen Energy **40**, 797 (2015).